Electronic Supplementary Material (ESI) for Physical Chemistry Chemical Physics.

Electronic Supporting Information: Strain-driven Phase Transition and Spin Polarization of Re-doped Transition-Metal Dichalcogenides

Rui-Ning Wang,[1,*] Chen-Dong Jin,[1] Hu Zhang,[1] Ru-Qian Lian,[1] Xing-Qiang Shi,[1] and Jiang-Long Wang[1,†]

[1] *Key Laboratory of Optic-Electronic Information and Materials of Hebei Province, National-Local Joint Engineering Laboratory of New Energy Photoelectric Devices, Key Laboratory of High-precision Computation and Application of Quantum Field Theory of Hebei Province, College of Physics Science and Technology, Hebei University, Baoding, 071002, P. R. China*

(Dated: March 8, 2021)

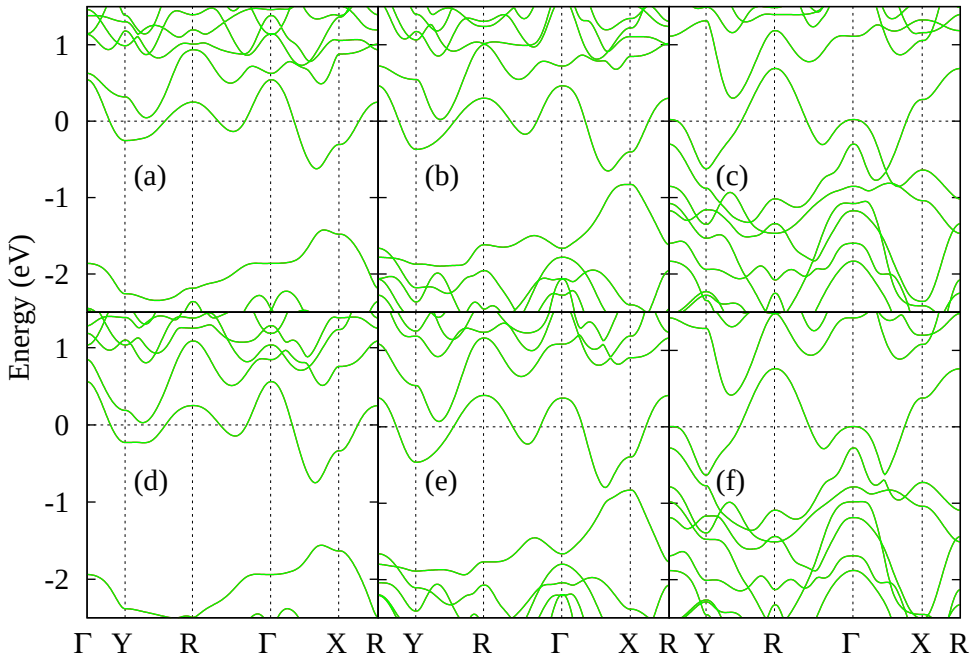

FIG. S1: (Color online). Calculated band structures of 1H-$Re_{0.5}M_{0.5}X_2$ monolayers without strain ((a) 1H-$Re_{0.5}Mo_{0.5}S_2$, (b) 1H-$Re_{0.5}Mo_{0.5}Se_2$, (c) 1H-$Re_{0.5}Mo_{0.5}Te_2$, (d) 1H-$Re_{0.5}W_{0.5}S_2$, (e) 1H-$Re_{0.5}W_{0.5}Se_2$, (f) 1H-$Re_{0.5}W_{0.5}Te_2$). The fermi level is set to zero.

Under strain-free conditions, all of 1H-$Re_{0.5}M_{0.5}X_2$ (M = Mo, W and X = S, Se, Te) monolayers show n-type character, but the spin-up and spin-down bands are symmetric. Thus, all of them are non-magnetic.

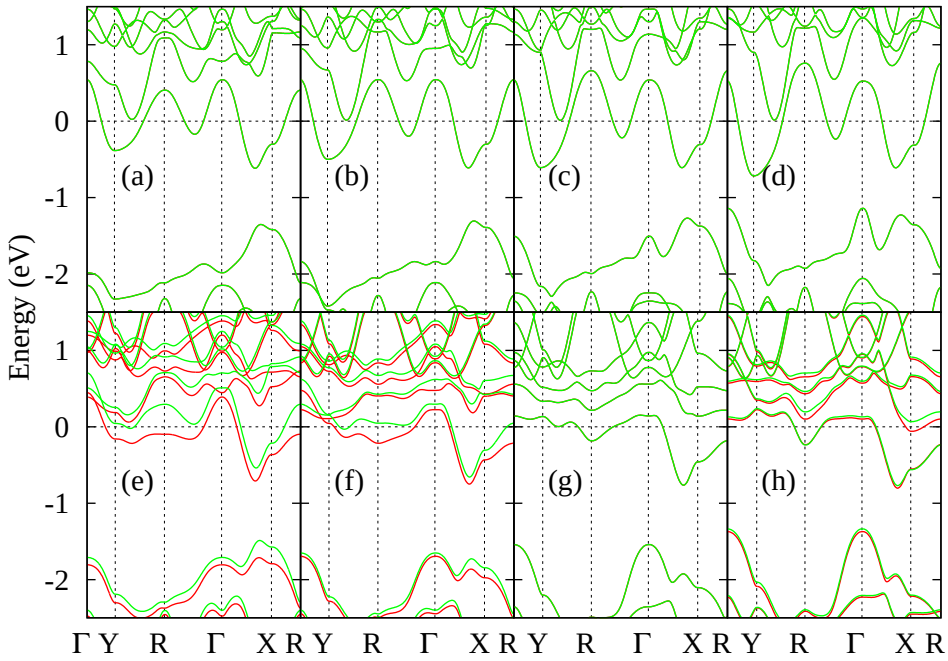

FIG. S2: (Color online). Calculated band structures of $1H$-$Re_{0.5}Mo_{0.5}S_2$ monolayer as a function of lattice constant $\vec{a}$ ((a) 3.078 Å, (b) 3.013 Å, (c) 2.950 Å, (d) 2.886 Å, (e) 3.206 Å, (f) 3.270 Å, (g) 3.335 Å, (h) 3.399 Å.) with a fixed $\vec{b}$=5.553 Å. The fermi level is set to zero. Red: Spin-up bands; Green: Spin-down bands.

For $1H$-$Re_{0.5}Mo_{0.5}S_2$ monolayers, their band structures as a function of lattice constant $\vec{a}$ with a fixed $\vec{b}$=5.553 Å are shown in Fig. S2. All conduction bands cross down the Fermi level, showing n-type characters. Furthermore, the spin-down and spin-up bands are always symmetric under uniaxial compressive strains ($\vec{a} < 3.142$ Å, (a-d)). That is, a uniaxial compressive strain does not induce magnetism. When the tensile strain ($\vec{a} = 3.206$ Å) is applied, the spin splitting between the spin-up and spin-down bands starts to appear. When the lattice constant $\vec{a}$ reaches to 3.335 Å, the splitting is sharply reduced and the magnetism will disappear.

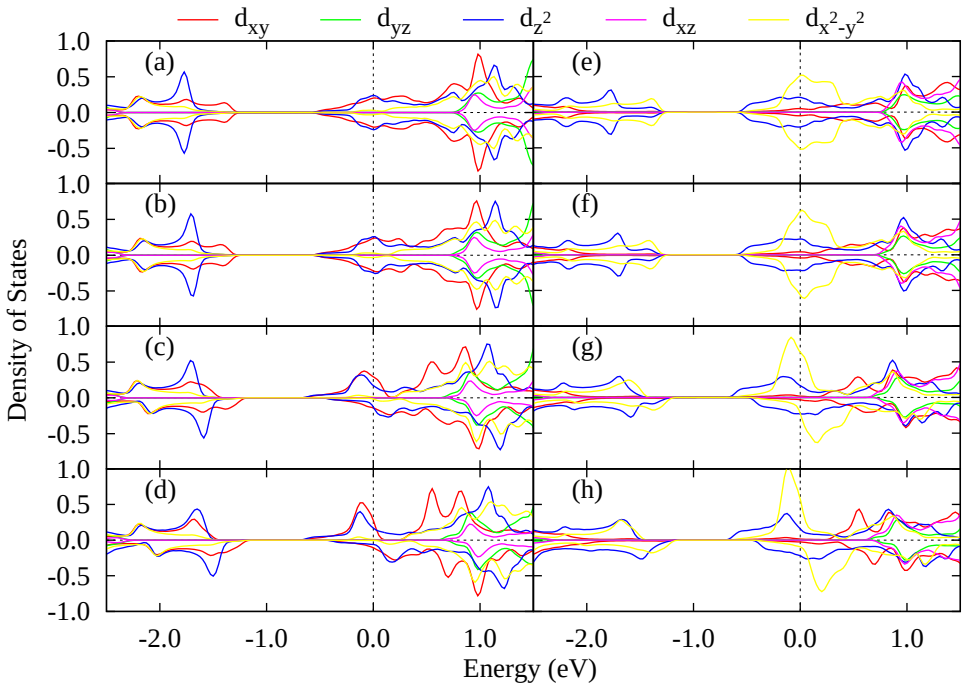

FIG. S3: (Color online). Calculated spin-polarized orbital projected density of states (DOS, (a-d) Mo and (e-h) Re) as a function of lattice constant $\vec{b}$ ((a,e) $\vec{b}$=5.553 Å, (b,f) $\vec{b}$=5.609 Å, (c,g) $\vec{b}$=5.665 Å, (d,h) $\vec{b}$=5.720 Å) for 1H-$Re_{0.5}Mo_{0.5}S_2$ with a fixed $\vec{a}$ = 3.142 Å. Positive and negative values represent the spin-up and spin-down DOS, respectively. The Fermi level is taken as zero.

With a fixed $\vec{a}$ = 3.142 Å, as a tensile uniaxial strain is applied to 1H-$Re_{0.5}Mo_{0.5}S_2$ along the $\vec{b}$ direction, the density of states around the Fermi level become narrower and narrower with increasing the tensile strain. As shown in Fig. S3(c, g), when $\vec{b}$=5.665 Å, the density of states begin to split, further leading to the magnetism appearing.

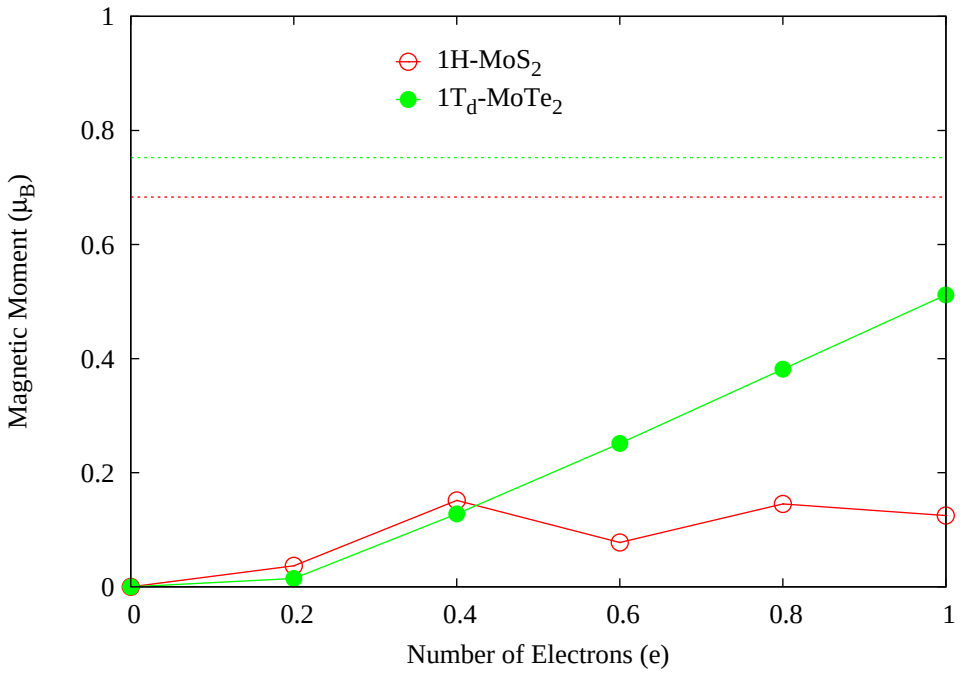

FIG. S4: (Color online). Calculated magnetic moments (μ_B) as a function of the additional virtual electrons for $1H$-MoS_2 with $\vec{a}$ = 3.142 Å and $\vec{b}$ = 5.887 Å and $1T_d$-$MoTe_2$ with $\vec{a}$ = 3.670 Å and $\vec{b}$ = 6.357 Å. Their corresponding magnetic moments for $1H$-$Re_{0.5}Mo_{0.5}S_2$ and $1T_d$-$Re_{0.5}Mo_{0.5}Te_2$ are indicated by dashed lines as the reference values.

Because Re doping will introduce one additional electron to MX_2 monolayers, we use the virtual electron approximation method to simulate the magnetic properties by Re doping. For monolayer $1H$-MoS_2 with $\vec{a}$ = 3.142 Å and $\vec{b}$ = 5.887 Å, Re doping induce 0.684 μ_B while one additional electron only induces the magnetic moment (0.125 μ_B). For monolayer $1T_d$-$MoTe_2$ with $\vec{a}$ = 3.670 Å and $\vec{b}$ = 6.357 Å, the magnetic moments are 0.753 μ_B and 0.512 μ_B for Re doping and one virtual electron doping, respectively.

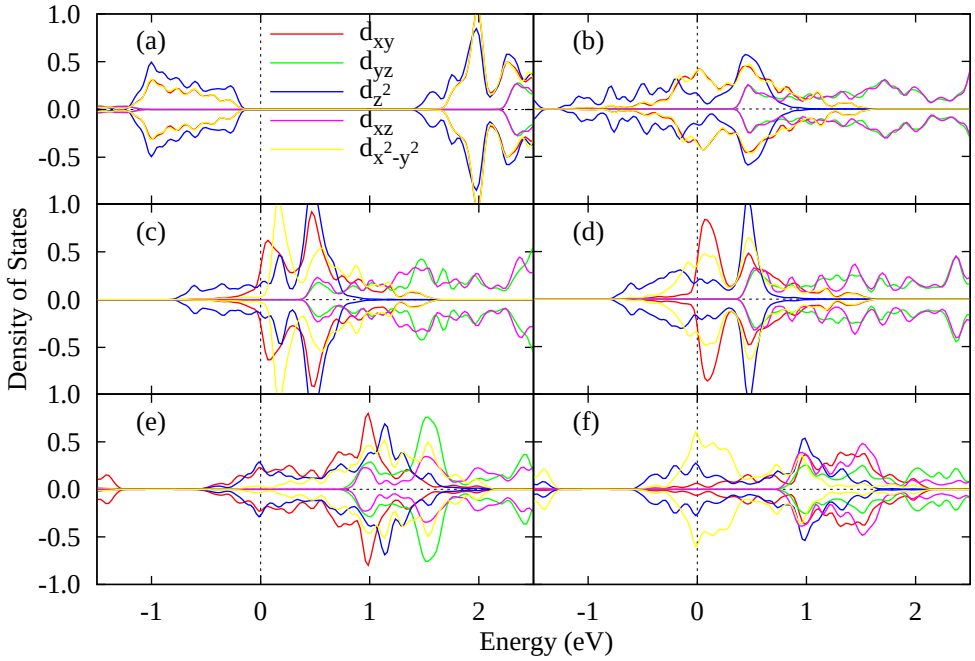

FIG. S5: (Color online). Calculated spin-polarized atomic orbital projected density of states (DOS) (a) 1H-MoS_2, (b) 1H-ReS_2, (c,d) 1H-$Re_{0.5}Mo_{0.5}S_2$ in a perfect hexagonal lattice, and (e,f) fully optimized 1H-$Re_{0.5}Mo_{0.5}S_2$ without strain. (a, c, e) and (b, d, f) panels indicate the Mo and Re atoms, respectively. Positive and negative values represent the spin-up and spin-down DOS, respectively. The Fermi level is taken as zero.

Fig. S5(a) gives the Mo atomic orbital projected density of states in pure 1H-MoS_2, showing one d_{z^2} orbit and two degenerate $d_{xy}/d_{x^2-y^2}$ orbits around the Fermi level. Fig. S5(b) gives the Re atomic orbital projected density of states in pure 1H-ReS_2, showing one d_{z^2} orbit and two degenerate $d_{xy}/d_{x^2-y^2}$ orbits through the Fermi level because one additional electron is doped. Fig. S5(c, d) give the Mo and Re atomic orbital projected density of states in 1H-$Re_{0.5}Mo_{0.5}S_2$ with a perfect hexagonal lattice (Mo at (0,0) site and Re at (0.5, 0.5) site), respectively. However, the original degenerate $d_{xy}/d_{x^2-y^2}$ orbits are split. For Mo atom, the d_{xy} orbit is closer to the Fermi level while the $d_{x^2-y^2}$ orbit of Re atom through the Fermi level. After full-optimization (Fig. S5(e, f)), the hexagonal lattice is broken, further leading to the d_{z^2} and d_{xy} orbits of Mo atom and the d_{z^2} and $d_{x^2-y^2}$ orbits of Re atom through the Fermi level.

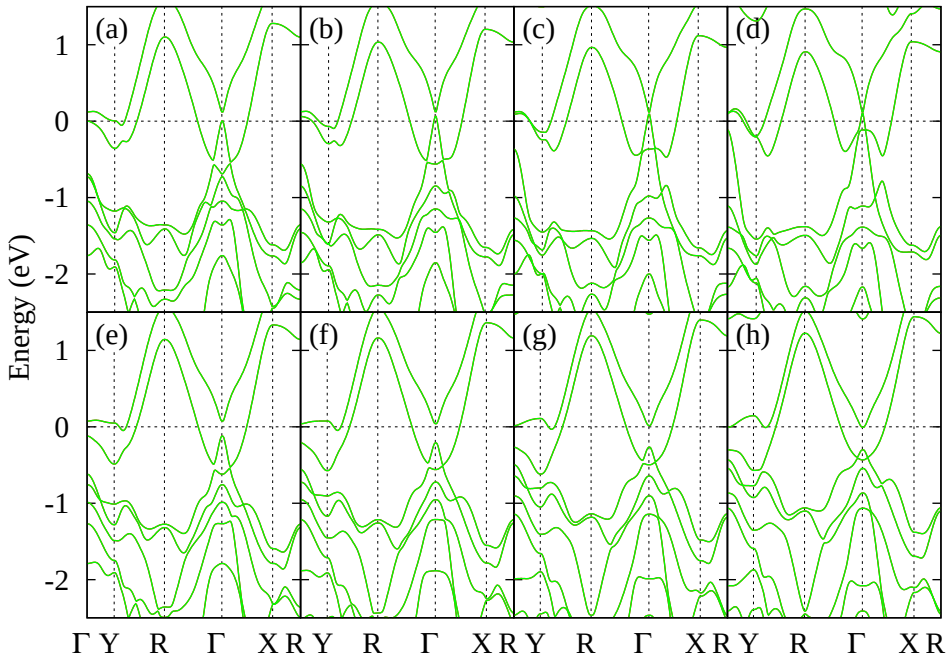

FIG. S6: (Color online). Calculated band structures of $1T_d$-$Re_{0.5}Mo_{0.5}S_2$ monolayers as a function of lattice constant $\vec{b}$ ((a) 5.609 Å, (b) 5.498 Å, (c) 5.387 Å, (d) 5.276 Å, (e) 5.776 Å, (f) 5.887 Å, (g) 5.998 Å, (h) 6.109 Å) with a fixed $\vec{a}$ = 3.142 Å. The fermi level is set to zero. Red: Spin-up bands; Green: Spin-down bands.

For $1T_d$-$Re_{0.5}Mo_{0.5}S_2$ monolayers, their band structures as a function of lattice constant $\vec{b}$ with a fixed $\vec{a}$=3.142 Å are shown in Fig. S6. All conduction bands cross down the Fermi level, showing n-type characters. Furthermore, the spin-down and spin-up bands are always symmetric. That is, a uniaxial compressive strain along the $\vec{b}$ direction does not induce magnetism.

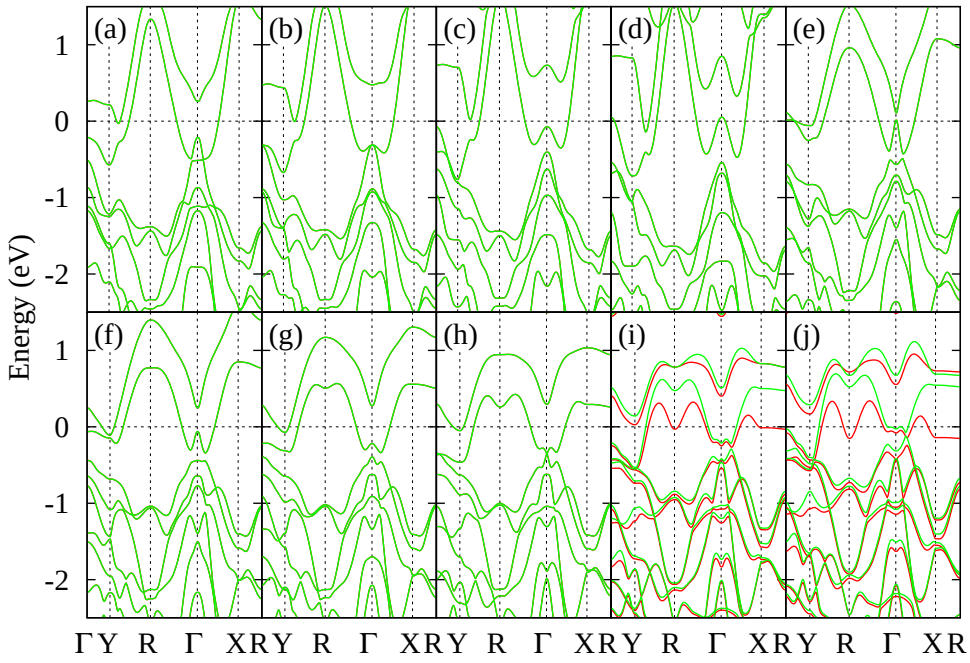

FIG. S7: (Color online). Calculated band structures of $1T_d$-$Re_{0.5}Mo_{0.5}S_2$ monolayers as a function of lattice constant $\vec{a}$ ((a) 3.078 Å, (b) 3.014 Å, (c) 2.950 Å, (d) 2.886 Å, (e) 3.206 Å, (f) 3.270 Å, (g) 3.335 Å, (h) 3.399 Å, (i) 3.463 Å, (j) 3.527 Å) with a fixed $\vec{b}$=5.720 Å. The fermi level is set to zero. Red: Spin-up bands; Green: Spin-down bands.

For $1T_d$-$Re_{0.5}Mo_{0.5}S_2$ monolayers, their band structures as a function of lattice constants $\vec{a}$ with a fixed $\vec{b} = 5.720$ Å are shown in Fig. S7. All conduction bands cross down the Fermi level, showing n-type character. Furthermore, the spin-down and spin-up bands are symmetric until a uniaxial tensile strain along the $\vec{a}$ direction reaches to $\sim 9.18\%$ ($\vec{a} = 3.463$ Å). On the contrary, a uniaxial compressive strain along the $\vec{b}$ direction seem to have no effect.

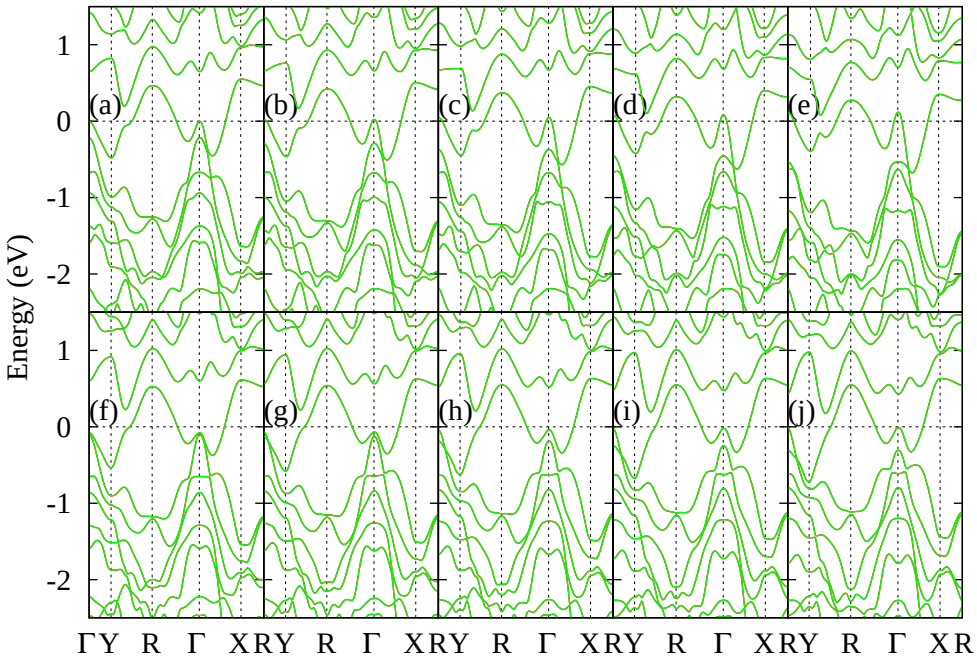

FIG. S8: (Color online). Calculated band structures of $1T_d$-$Re_{0.5}Mo_{0.5}Te_2$ monolayers as a function of lattice constant $\vec{b}$ ((a) 6.296 Å, (b) 6.235 Å, (c) 6.174 Å, (d) 6.113 Å, (e) 6.052 Å, (f) 6.418 Å, (g) 6.480 Å, (h) 6.541 Å, (i) 6.602 Å, (j) 6.663 Å) with a fixed $\vec{a}$=3.459 Å. The fermi level is set to zero. Red: Spin-up bands; Green: Spin-down bands.

For $1T_d$-$Re_{0.5}Mo_{0.5}Te_2$ monolayers, their band structures as a function of lattice constant $\vec{b}$ with a fixed $\vec{a} = 3.459$ Å are shown in Fig. S8. All the spin-down and spin-up bands are always symmetric, when a uniaxial compressive strain along the $\vec{b}$ direction is applied.

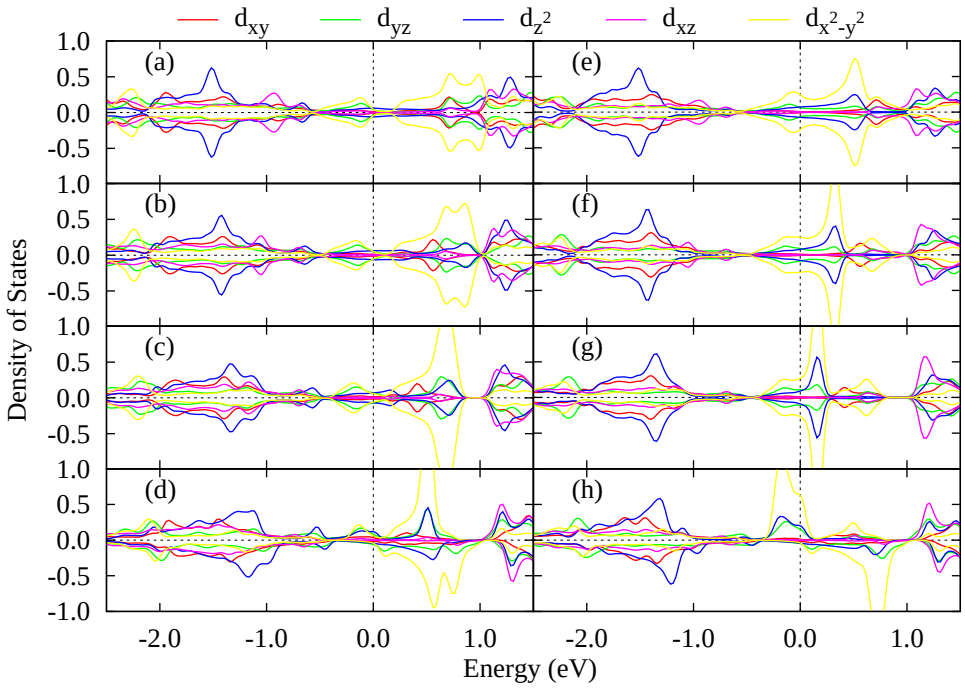

FIG. S9: (Color online). Calculated spin-polarized atomic projected density of states ((a-d) Mo and (e-h) Re) as a function of lattice constant $\vec{a}$ ((a,e) $\vec{a}$=3.459 Å, (b,f) $\vec{a}$=3.529 Å, (c,g) $\vec{a}$=3.600 Å, (d,h) $\vec{b}$=3.670 Å) for 1T_d-$Re_{0.5}Mo_{0.5}Te_2$ with a fixed $\vec{b}$ = 6.357 Å. Positive and negative values represent the spin-up and spin-down bands, respectively. The Fermi level is taken as zero.

For 1T_d-$Re_{0.5}Mo_{0.5}Te_2$, the conduction bands of Re atoms move to the Fermi level and become narrower and narrower when a uniaxial tensile strain is applied along the $\vec{a}$ direction. Finally, the conduction bands around the Fermi level are mainly contributed by Re's $d_{x^2-y^2}$, d_{z^2} and d_{yz}. Therefore, at a certain tensile strain, the magnetic moments are mainly attributed to these three orbits.

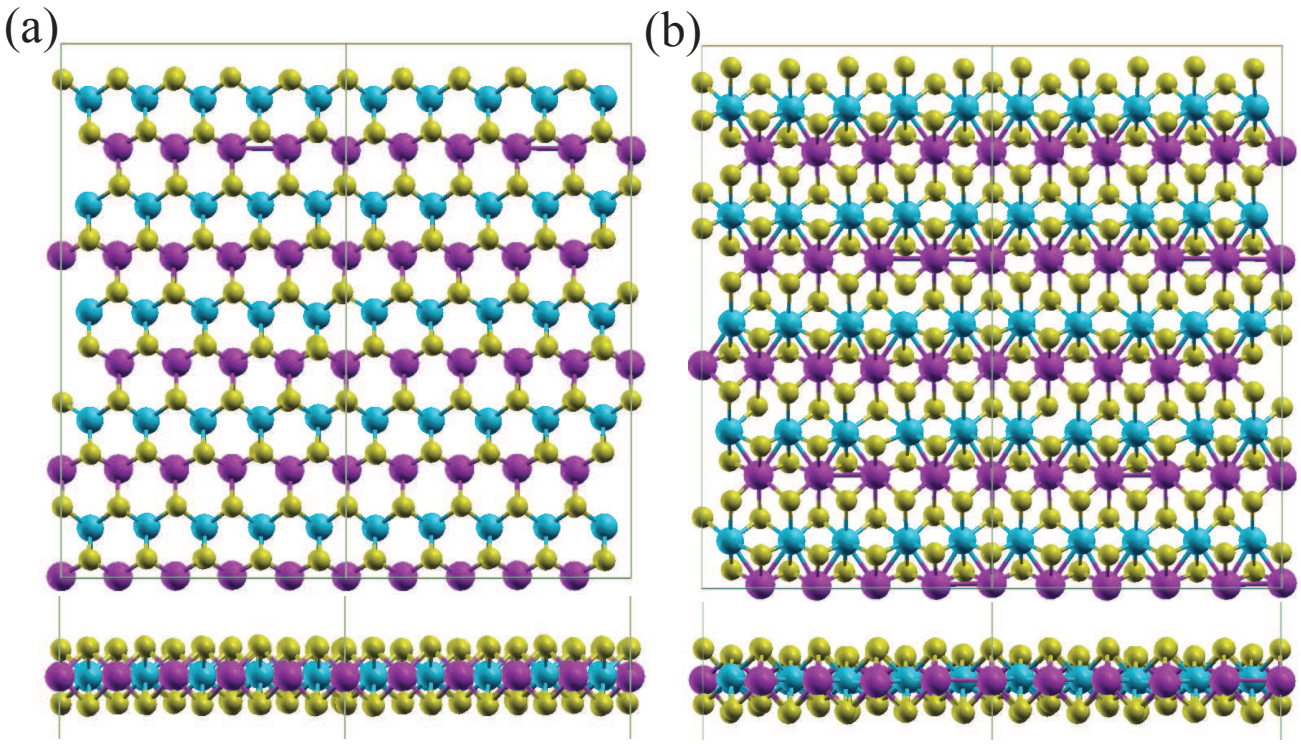

FIG. S10: (Color online). Top and side views of fully-optimized (a) $1H$- and (b) $1T_d$-$Re_{0.5}Mo_{0.5}S_2$ monolayers with $\vec{a} = 3.142$ Å and $\vec{b} = 5.887$ Å. Mo atoms, Pink; S atoms, yellow; Re atoms, blue.

Taking monolayer $1H$- and $1T_d$-$Re_{0.5}Mo_{0.5}S_2$ with $\vec{a} = 3.142$ Å and $\vec{b} = 5.887$ Å as examples, we do first-principles molecular dynamics simulations at 300 K. It is find that within up to 1 ps (the step size 1 fs) Re-doped $Mo_{0.5}S_2$ are thermodynamically stable. The corresponding structures are shown in Figs. S10 (a,b).

* Electronic address: rnwang@hbu.edu.cn
† Electronic address: jlwang@hbu.edu.cn